

See discussions, stats, and author profiles for this publication at: <https://www.researchgate.net/publication/51834286>

High-Yield Production of Long Branched Au Nanoparticles Characterized by Atomic Resolution Transmission Electron Microscopy

ARTICLE *in* CRYSTAL GROWTH & DESIGN · OCTOBER 2011

Impact Factor: 4.89 · DOI: 10.1021/cg2007638 · Source: PubMed

CITATIONS

7

READS

30

3 AUTHORS, INCLUDING:



[César Magén](#)

University of Zaragoza

173 PUBLICATIONS 2,235 CITATIONS

[SEE PROFILE](#)



[Miguel Jose Yacaman](#)

University of Texas at San Antonio

466 PUBLICATIONS 10,529 CITATIONS

[SEE PROFILE](#)



NIH Public Access

Author Manuscript

Cryst Growth Des. Author manuscript; available in PMC 2012 October 5.

Published in final edited form as:

Cryst Growth Des. 2011 October 5; 11(10): 4538–4543. doi:10.1021/cg2007638.

High yield production of long branched Au nanoparticles characterized by atomic resolution transmission electron microscopy

Alvaro Mayoral¹, Cesar Magen^{1,2,3}, and Miguel Jose-Yacaman^{4,*}

¹Laboratorio de Microscopías Avanzadas (LMA), Instituto de Nanociencia de Aragón (INA), Universidad de Zaragoza, 50018 Zaragoza, Spain

²Departamento de Física de la Materia Condensada, Universidad de Zaragoza, 50009 Zaragoza, Spain

³Fundación ARAID, 50004 Zaragoza, Spain

⁴Department of Physics and Astronomy, The University of Texas at San Antonio, One UTSA Circle, 78251 San Antonio, Texas, USA

Abstract

Long multi-branched gold nanoparticles have been synthesized in a very high yield through a facile synthesis combining two different capping agents. The stability of these materials with the time has been tested and their characterization have been performed by diverse advanced electron microscopy techniques, paying special attention to aberration corrected transmission electron microscopy in order to unambiguously analyze the surface structure of the branches and provide insights for the formation of stellated gold nanoparticles.

INTRODUCTION

Noble metal nanoparticles (NP's) have attracted lot of interest because of the different electromagnetic, optical, and physicochemical properties that they exhibit depending on their size, shape and composition. The applications in different fields such as cancer therapy, drug delivery, surface enhanced Raman spectroscopy or biological labelling are currently being exploited^{1–10} and, as a consequence, a great effort is continuously being devoted into the production of these materials. Controlling the size, shape and the production of different morphologies such as rods^{1–11}, cubes^{12,13}, stars^{14,15} or branched crystals^{16–20} is crucial for the practical use of these materials. Among all applications, surface Raman spectroscopy^{19,21}, where dendritic nanoparticles^{22–24} receive and enormous interest, and cancer therapy research^{2,25} are the most attractive fields and, for this purpose, materials which absorb the energy near the infrared zone are required. At this wavelength, human tissue and fluids are highly transmissive²⁶ and by applying the right energy, gold nanoparticles can act as markers for cancer cells as they appear illuminated with respect to the cells or even act as nanoheaters for cancer cell photothermal therapy²⁷.

In this context, branched NP's are advantageous respect to nanowires as the present a more suitable geometry for a better cell-nanoparticle interaction. In addition, the absorption spectra can be tune depending on the size and shape of their peaks^{1,14,19,28}. However, due to the highly symmetric face-centered cubic (*fcc*) structure of noble metals such as Ag, Pt or Au,

*Miguel.yacaman@utsa.edu. Phone +1 210 4585451, Fax +1 210.458.4919.

the production of anisotropic nanocrystals has resulted a challenge recently overcome by the presence of templates or capping agents. Cetyl trimethylammonium bromide (CTAB) has been widely employed because of the great diversity of morphologies than can be obtained. Pluronic triblock copolymers composed of poly(ethylene oxide)-*block*-poly(propylene oxide)-*block*-poly(ethylene oxide) (PEO-PPO-PEO) have been also used for the stabilization of metal nanoparticles in a similar way as CTAB^{29–33}. In the present work, a combination of both surfactants CTAB and Pluronic block copolymer F-127 (PEO₁₀₆PPO₇₀PEO₁₀₆) have been employed based on our previous synthesis of gold nanostars^{14,15} to finally produce a high yield of long branched gold nanoparticles. The morphology of the crystals has been characterized by scanning electron microscopy (SEM). Moreover, an atomic resolution observation of the surface defects of the tips of the branches by means of transmission electron microscopy (TEM) is also presented showing the “in-situ” surface reconstruction and proving the stability of certain facets.

EXPERIMENTAL SECTION

All the chemicals were purchased from Sigma Aldrich and BASF (pluronic F-127) and used without further purification.

Synthesis

Preparation of Silver Seeds—25 mL aqueous solution of 2.5×10^{-4} M AgNO₃ was mixed with 25 mL of 2.5×10^{-4} M Trisodium Citrate. Subsequently, 0.6 mL of 0.1M NaBH₄ was rapidly added to this solution (an immediate colour change to a dark-green/yellow was observed). The silver solution was kept under static conditions for few hours before being used for nanoparticle growth.

Preparation of Gold Nanoparticles—An aqueous solution of 1.25×10^{-3} M CTAB (10 mL) was heated and stirred until CTAB was completely dissolved. Immediately after removing the heat source, 5 mL of 2.5×10^{-4} M HAuCl₄ was added, forming an orange-red mixture. To this mixture 10 mL of 1.25×10^{-4} M F-127 Pluronic were added and let under vigorous stirring for 5 minutes. Subsequently, the gold ions were reduced with the addition of 0.7 mL of ascorbic acid, 1M. After that, 12.5 μL solution of silver seeds were added into the reaction mixture. The finished nanoparticles were then stirred for at least 30 minutes.

Characterization

UV-visible absorption spectra in the range of 450–1100 nm were obtained with Agilent 8453 UV-Visible Spectrophotometer.

Before electron microscopy analysis, the product was washed several times, centrifuged at 3000 rpm and finally dispersed in distilled water to minimize the amount of surfactant which could remain coating the crystals. Scanning electron microscopy (SEM) was performed in a FEG Hitachi S-5500 ultrahigh resolution electron microscope (0.4 nm resolution at 30 kV) with BF/DF Duo-STEM detector. Bright field (BF) transmission electron microscopy (TEM), selected area electron diffraction (SAED), weak beam dark field (WBDF) and X rays energy dispersive spectroscopy (EDS) analyses were performed using a JEOL 2010F with a point-to-point resolution of 0.23 nm. Aberration corrected high resolution TEM was performed on a FEI TITAN Cube 60–300 equipped with an aberration corrector for the objective lens and operated at 300 kV.

For this TEM analysis, a drop of the suspension previously centrifuged was put onto a holey carbon Cu microgrid and let to dry.

RESULTS AND DISCUSSION

Figure 1 displays the low and high magnification SEM images of the as-synthesized product. The final Au product is composed by nanoparticles which for almost every case developed branches with high aspect ratio (Figure 1a inset). The yield of branched nanoparticles was very high reaching 90% and the reproducibility was tested by repeating the entire process several times obtaining in every case the same type of material and high yield.

In the present synthesis the pluronic surfactant plays a key role on the formation of the long branches as in the absence of this reactant only star-shaped nanoparticles were obtained¹⁵. In addition, it should be stressed that this anisotropic nanostructures are remarkable stable at room temperature as no significant changes were observed 10 months after synthesis.

The importance of the presence of the F-127 surfactant was confirmed by repeating the reaction in the absence of it^{14,15}. This reactant is composed by two chains of PEO linked by 70 PPO units. These units are hydrophobic and in a water media they tend to form micelles. However, in our case the pluronic concentration was below the critical micelle concentration (CMC)³⁴. Therefore, it is expected that the hydrophobic groups were adsorbed onto the gold surfaces³² leading into the formation of long branches in a similar fashion as occurred for the production of gold nanowires³³, see figure 2.

As a consequence of the multiple long branches, the UV-Vis spectra exhibited adsorption bands almost in the near-infrared (NIR) region. The UV-Vis spectrum, figure 1b, shows the observed optical absorption spectra of the as-synthesized sample. The adsorption bands of the gold nanoparticles can be centered at 820 nm and 980 nm, which can be assigned to tips of the branched as a result of the longitudinal oscillation of electrons. The longitudinal long-wavelength absorption band is sensitive to the one-dimensional nanomaterials aspect ratios. It usually shifts to the NIR region as the aspect ratio increases³⁵. The appearance of two major absorption bands can be attributed to the different sizes of nanostar tips and the different polarization angles^{36–38} (which according to Link *et al.*³⁸ would correspond to aspect ratios of 5.6 for 980 nm and 4.1 for 820 nm) in combination with the transversal, 820 nm, and the longitudinal plasmon modes, 980 nm.

TEM imaging together with the Fast Fourier Transform (FFT) analysis revealed that the peak growth occurred in two ways: through the formation of a defect in the middle of the branch or forming a complete single crystal structure with no structural defects. Both cases are illustrated in Figure 3. Figure 3 represents a stellated gold nanoparticle (similar to the original product obtained when Pluronic surfactant was absent in synthesis¹⁴) with the symmetry broken due to the formation of a long branch. Figure 3a corresponds to the weak beam dark field (WBDF) image using the (200) diffracted spot, after tilting several degrees, where contour lines related to the thickness of the crystal can be easily identified. The fact that no contrast changes were observed on the majority of the particle indicates that it forms a single crystal structure free of defects until the appearance of the branch which grows containing a defect in the middle of it. Furthermore, another two (almost perpendicular) defects can be observed. Interestingly, it is remarkable that the formation of defects in the structure was observed in branches that grew along the <110> direction³⁹. The high-resolution TEM analysis confirmed the formation of multiple stacking faults along the entire branch; Figure 3b displays the atomic resolution image of the tip of the peak with the FFT inset, where the streaked structure of spots perpendicular to the branch is due to the presence of defects. Figure 3c displays a similar TEM analysis performed on a gold single crystal. The WBDF, using the (220) diffracted spot, reveals no defects. This is also confirmed by the FFT and the HRTEM analysis and it may be related to a kinetically controlled growth^{12,40}.

For the single crystal structure the branches grew along the <111> direction in agreement with the original star-shaped nanoparticle¹⁵. FFT is indexed assuming the *fcc* bulk structure of gold (*Fm-3m* see Fig. 3d).

To study the composition of the branched nanoparticles, TEM EDS was employed. Figure 4 shows the TEM-EDS data taken on the core, white rectangle marked as 1 and on the branch, white rectangle, marked as 2. The EDS spectra are presented in Figure 4b, both of them clearly show the Au peaks in the core and in the branch; the Ag signal is significantly lower and it is virtually the same in the core and in the branch suggesting that the Ag diffused along the crystal in agreement with the data reported by Zhang et al.³⁹ in pentagonal bipyramids. This evidence is also supported by the WBDF data, where if the Ag seeds was present it should be observed¹⁴.

With the purpose of gaining detailed information on the peak growth and surface formation, aberration corrected HRTEM experiments were performed on a free-surfactant branch. With this technique it is possible to eliminate delocalization, which is always present in a conventional TEM as a consequence of the spherical aberration coefficient different from zero, and sharper images of the surfaces can be obtained where the positions of the last atomic columns can be unambiguously determined. Moreover, atomic displacement can be accurately measured as the images are not blurred by this effect.

In order to relax the surface energy, steps on the surface were formed along the long peaks. Figure 5a shows the high-resolution image of one of the sides of a branch from a standard gold nanoparticle (shown inset). Monoatomic surface steps (marked with white arrows on Figure 5a) are present along the entire branch, which grows along the <110> direction, being responsible for the narrower size of the tip. In addition to the formation of the surface steps, a mismatch on the atomic positions has been observed on the last two atomic layers of the edges where the monoatomic steps take place. An atomic displacement of 20% to 35% respect to the theoretical position has been measured⁴¹, figure 5c, marked by white lines. The presence of steps and the atomic displacement may be responsible for the stabilization of the energetic unfavorable {110} facet⁴². We also noticed the presence of a twin boundary across the middle of the peak. This boundary divides the peak in two halves.

The tip of the peak presents extra {111} and {100} facets giving roundness to the structure^{43,44}. These facets are energetically more stable than the {110} and are predicted to be predominant over the {110} facet. However, the presence of a surfactant (two in the present study) may be responsible for the branch growth⁴⁴ direction. On the tip the most stable facets on a *fcc* symmetry are forming the edge, see Figure 5b and Figure 6. Figure 6 displays a sequence that shows the in-situ surface reconstruction of the {111} facet. The formation of monoatomic steps Au(S)-2(111) × (111) are marked by white arrows in Figures 6b and 6d, in both sides of the last monoatomic layer and in Figure 6f on the bottom side of the atomic layer, similar to those formed on Pt nanoparticles⁴¹. This atomic rearrangement occurred during 140 seconds of observation and after that time, an entire {111} facet was formed and remained stable confirming the energetically favorable formation of this facet^{42,41}. It is very likely that the atomic reconstruction was induced by the electron beam. The origin of the extra atoms in fig 6 is not clear but most likely is coming from the top of the last row of atoms.

CONCLUSION

In summary, in the present manuscript we have demonstrated that the combination of two surfactants can be employed to synthesize multibranched gold nanoparticles by a simple method. The yield obtained has been higher than 95% of nanoparticles that developed

ultralong branches and the reproducibility has been tested repeating the reaction several times. At macroscopic scale, this gold multibranched nanostructures has an optical response suitable for applications, as two main absorption bands close to the NIR range, at wavelengths of 820 nm and 980 nm.

The structure at atomic level has been analysed by different advanced transmission electron microscopy techniques observing the formation of two kinds of nanoparticles depending on the growth direction of the branch: faulty branches when grown along $<110>$, or forming a single crystal with (111) branches suggesting the strong relationship between the actual morphology and the presence of an extra surfactant. Curved tip of the branches was caused by atomic steps and multiple faceting along $<100>$, $<110>$ and $<111>$. Furthermore, in-situ surface reconstruction was observed by means of Cs corrected HRTEM, technique that avoids delocalization on the surface.

Acknowledgments

Part of this work was supported by Award Number 2G12RR013646-11 from the National Center For Research Resources. The content is solely the responsibility of the authors and does not necessarily represent the official views of the National Institute of Health. The authors would like to thank Dr. Weijia Zhang for useful discussions.

REFERENCES

1. Murphy CJ, Sau TK, Gole AM, Orendorff CJ, Gao J, Gou L, Hunyadi SE, Li T. *J. Phys. Chem. B.* 2005; 109:13587–13870.
2. Perrault SD, Walkey Cl, Jennings T, Fischer HC, Chan WCW. *Nano Lett.* 2009; 9:1909–1915. [PubMed: 19344179]
3. Sun L, Liu D, Wang Z. *Langmuir*. 2008; 24:10293. [PubMed: 18715022]
4. Surbhi L, Susan CE, Halas NJ. *Acc. Chem. Res.* 2008; 41:1842–1851. [PubMed: 19053240]
5. Hao E, Bailey RC, Schatz GC, Hupp JT, Li S. *Nano Lett.* 2004; 4:327–330.
6. Bakr OM, Wunsch BH, Stellacci F. *Chem. Mater.* 2006; 18:3297–3301.
7. Haes AJ, Hall WP, Chang L, Klein WL, Duyne RPV. *Nano Lett.* 2004; 4:1029–1034.
8. Zhang W, Liu Y, Cao R, Li Z, Zhang Y, Tang Y, Fan K. *J. Am. Chem. Soc.* 2008; 130:15581–15588. [PubMed: 18950178]
9. Zhang W, Chen P, Gao Q, Zhang Y, Tang Y. *Chem. Mater.* 2008; 20(5):1699–1704.
10. Cabrera-Trujillo JM, Montejano-Carrizales JM, Rodriguez-Lopez JL, Zhang W, Velazquez-Salazar JJ, Jose-Yacaman M. *J. Phys. Chem. C.* 2010; 114:21051–21060.
11. Kim F, Song JH, Yang PD. *J. Am. Chem. Soc.* 2002; 124:14316–14317. [PubMed: 12452700]
12. Sau TK, Murphy CJ. *J. Am. Chem. Soc.* 2004; 126:8648–8649. [PubMed: 15250706]
13. Shankar SS, Rai A, Ankamwar B, Singh A, Ahmad A, Sastry M. *Nat. Mater.* 2004; 3:482–488. [PubMed: 15208703]
14. Mayoral A, Vazquez-Duran A, Barron H, Jose-Yacaman M. *Appl. Phys. A.* 2009; 97:11–18.
15. Mayoral A, Vazquez-Duran A, Ferrer D, Montejano-Carrizales JM, José-Yacamán M. *CrystEngComm.* 2010; 12:1090–1095.
16. Chen S, Wang ZL, Ballato J, Foulger SH, Carroll DL. *J. Am. Chem. Soc.* 2003; 125:16186–16187. [PubMed: 14692749]
17. Guo S, Wang L, Dong S, Wang E. *J. Phys. Chem. C.* 2008; 112:13510–13515.
18. Lu L, Ai K, Ozaki Y. *Langmuir*. 2008; 24:1058–1063. [PubMed: 18177060]
19. Khouri CG, Vo-Dinh T. *J. Phys. Chem. C.* 2008; 112:18849–18859.
20. Li Z, Li W, Camargo PHC, Xia Y. *Angew. Chem. Int. Ed.* 2008; 47:9653.
21. Esenturk EN, Walker ARH. *J. Raman Spectrosc.* 2009; 40:86–91.
22. Fang J, Ma X, Cai H, Song X, Ding B. *Nanotechnology*. 2006; 17:5841–5845.
23. Fang J, Du S, Lebedkin S, Li Z, Kruk R, Kappes M, Hahn§ H. *Nano Lett.* 2010; 10:5006–5013.

24. Fang J, You H, Kong P, Yi Y, Song X, Ding B. *Crystal Growth & Design*. 2007; 7:864–867.
25. Lal S, Clare SE, Halas NJ. *Acc. Chem. Res.* 2008; 41:1842–1851. [PubMed: 19053240]
26. Weissleder RA. *Nat. Biotechnol.* 2001; 19:316–317. [PubMed: 11283581]
27. Elliott AM, Stafford RJ, Schwartz J, Wang J, Shetty AM, Bourgoine C, O'Neal P, Hazle JD. *Med Phys.* 2007; 34:3102–3108. [PubMed: 17822017]
28. Nehl CL, Liao H, Hafner JH. *Nano Lett.* 2006; 6:683–688. [PubMed: 16608264]
29. Rahme K, Gauffre F, Marty JD, Payre B, Mingotaud C. *J. Phys. Chem. C*. 2007; 111:7273–7279.
30. Rahme K, Oberdisse J, Schweins R, Gaillard C, Marty JD, Mingotaud C, Gauffre F. *ChemPhysChem*. 2008; 9:2230–2236. [PubMed: 18821541]
31. Ataee-Esfahani H, Wang L, Yamauchi Y. *Chem. Comm.* 2010; 46:3684–3686. [PubMed: 20393665]
32. Wang L, Yamauchi Y. *J. A. Chem. Soc.* 2009; 131:9152–9153.
33. Iqbal M, Chung YI, Tae G. *J. Mater. Chem.* 2007; 17:335–342.
34. Sakai T, Alexandridis P. *Langmuir*. 2004; 20:8426–8430. [PubMed: 15379456]
35. Huang X, El-Sayed IH, Qian W, El-Sayed MA. *J. Am. Chem. Soc.* 2006; 128:2115–2120. [PubMed: 16464114]
36. Hao F, Nehl CL, Hafner JH, Nordlander P. *Nano Lett.* 2007; 7(3):729–732. [PubMed: 17279802]
37. N'Gom M, Ringnalda J, Mansfield JF, Agarwal A, Kotov N, Zaluzec NJ, Norris TB. *Nano Lett.* 2008; 8:3200–3204. [PubMed: 18778109]
38. Link S, El-Sayed MA. *J. Phys. Chem. B*. 1999; 103:8410–8426.
39. Zhang X, Tsuji M, Lim S, Miyamae N, Nishio M, Hikino S, Umez M. *Langmuir*. 2007; 23:6372–6376. [PubMed: 17469858]
40. Lou XW, Yuan C, Archer LA. *Chem. Mater.* 2006; 18:3921–3923.
41. Chang LY, Barnard AS, Gontard LC, Dunin-Borkowski RE. *Nano Lett.* 2010; 10:3073–3076. [PubMed: 20666362]
42. Hakkinen H, Merikoski J, Manninen M. *J. Phys.: Condens. Matter*. 1991; 3:2755–2767.
43. Jose-Yacaman M, Ascencio JA, Canizal G. *Surf. Sci.* 2001; 486:449–453.
44. Wang ZL, Gao RP, Nikoobakht B, El-Sayed MA. *J. Phys. Chem. B*. 2000; 104:5417–5420.
45. Grzelczak M, Pérez-Juste J, Mulvaney P, Liz-Marzán LM. *Chem. Soc. Rev.* 2008; 37:1783–1791. [PubMed: 18762828]

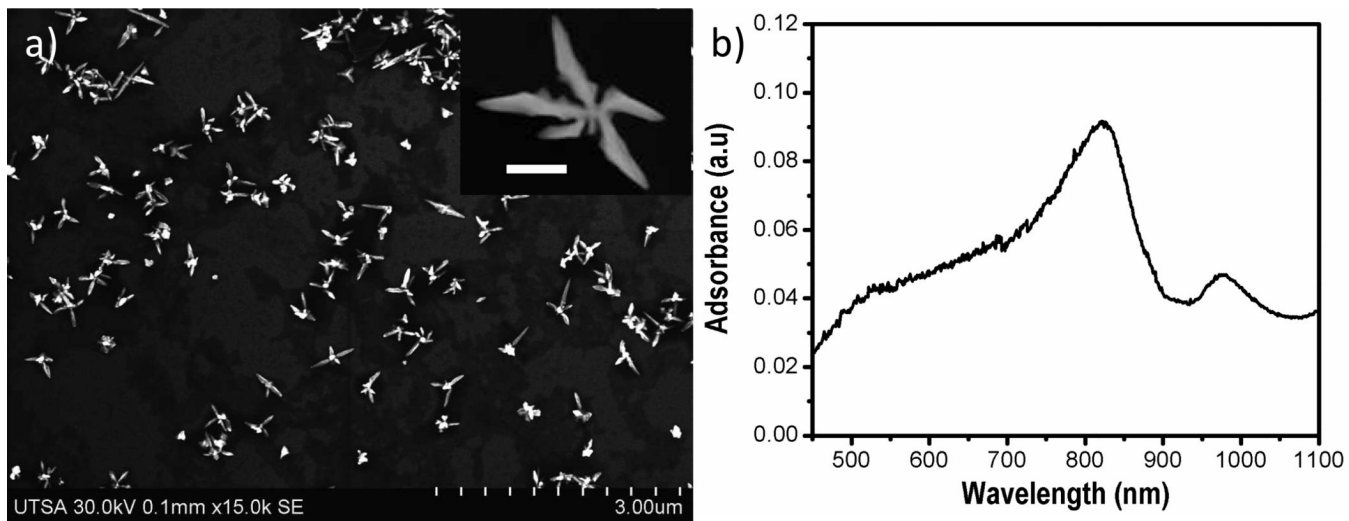


Figure 1.

a) Low magnification SEM image of the as-synthesized product where several agglomerated nanoparticles can be observed. Inset the Electron microscopy image taken on the SEM equipment using the dark field collector of an isolated nanoparticle, scale bar 100nm. b) UV-vis spectra of the assynthesized product, showing the two edges at 820 and 980 nm.

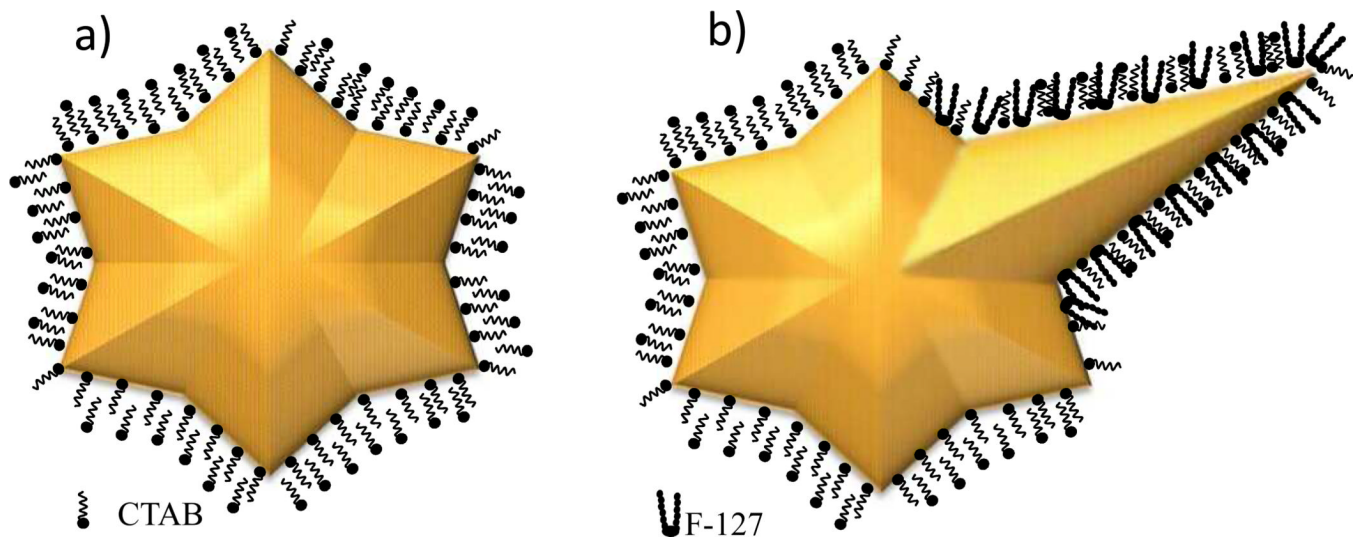
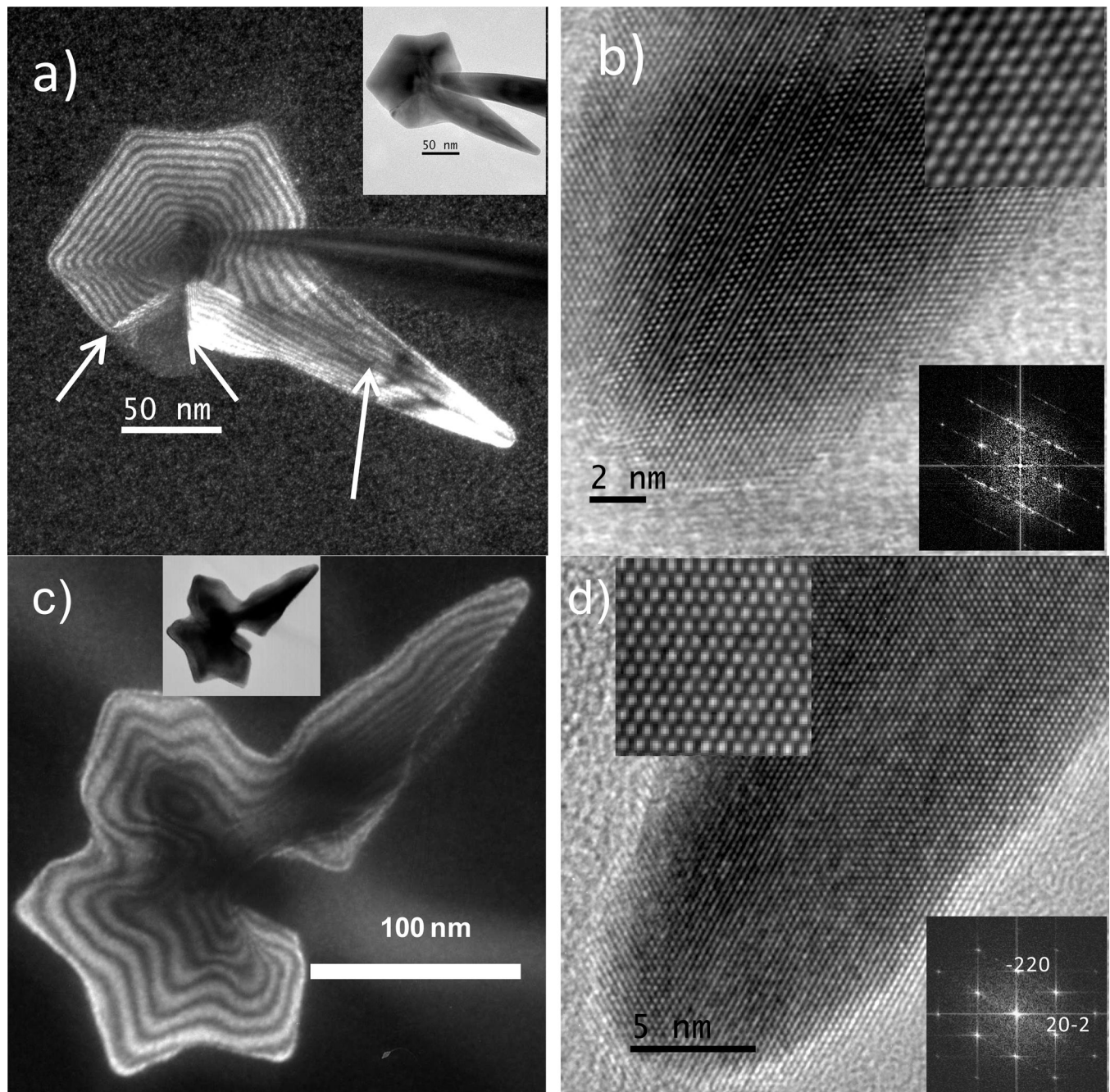


Figure 2.

Schematic cartoon showing the nanomaterials obtained in the absence and presence of pluroin surfactant. a) Original gold nanoparticle^{14,15} coated with a CTAB bilayer⁴⁵ and b) resulting branched nanoparticle stabilized with CTAB and F-127³³.

**Figure 3.**

a) WBDF TEM image using the {200} reflection of a gold “nanostar” which has developed a long peak of approximately 120 nm. The defects are marked by white arrows and the BF image is shown inset. b) HRTEM image of the tip of the branch with an enlarged atomic distribution image and the FFT shown inset. c) WBDF TEM image using the {220} reflection of a gold monocrystal (no defects were observed) BF is shown inset. d) The HRTEM image of the tip; the FFT diffractogram and the atomic distribution are shown inset.

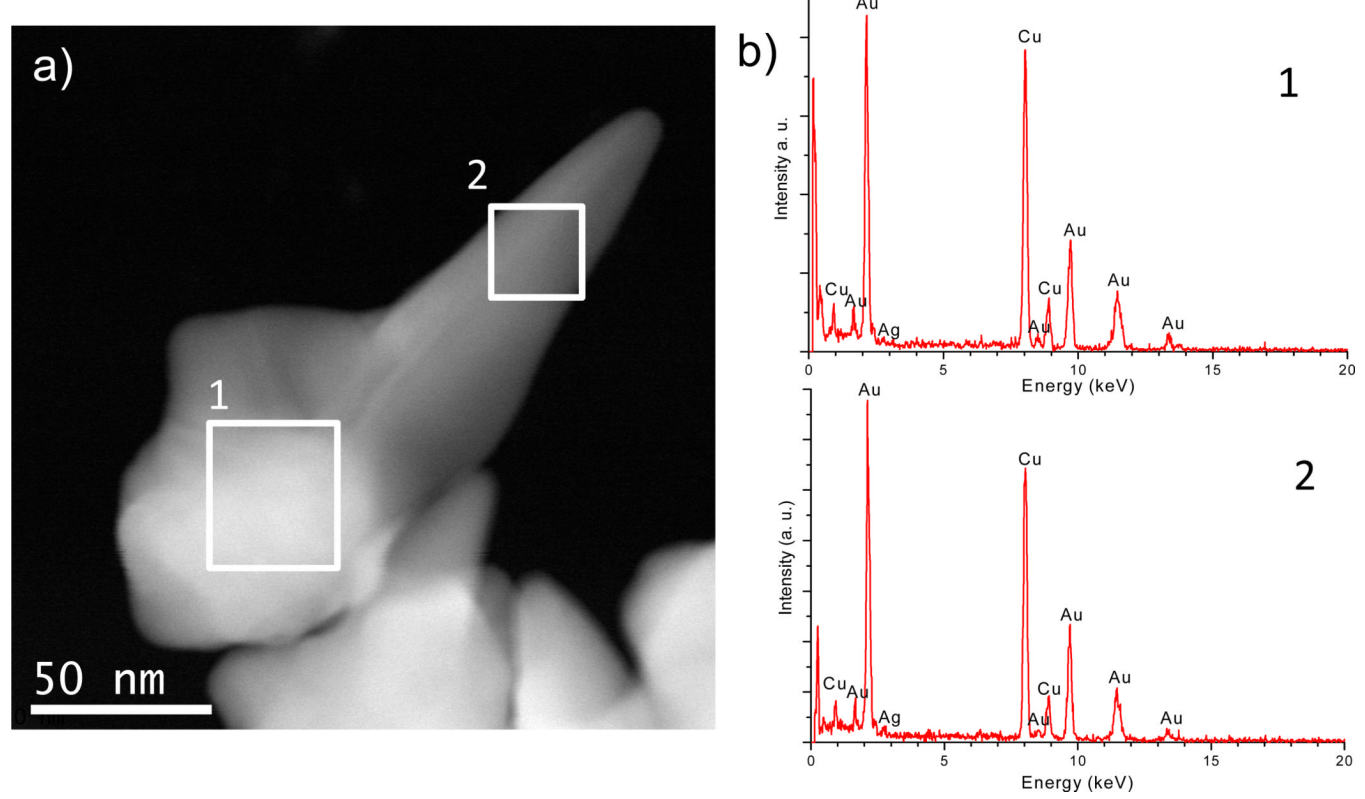


Figure 4.

TEM EDS data of a branched nanoparticle performed at the core, 1, and on the branch, 2.

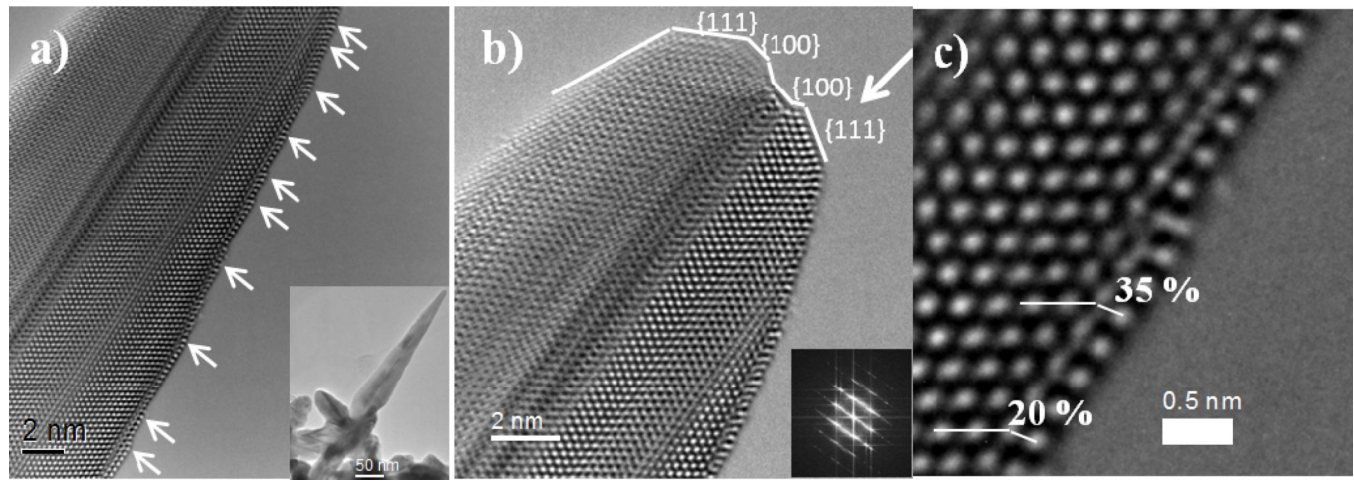


Figure 5.

Aberration corrected HRTEM images of a branch emerging from a gold nanoparticle. a) Monoatomic steps marked by arrows; the entire particle is shown inset. b) Tip of the branch where the different facets are marked. c) Atomic resolution image of a monoatomic step where the atomic displacement is marked

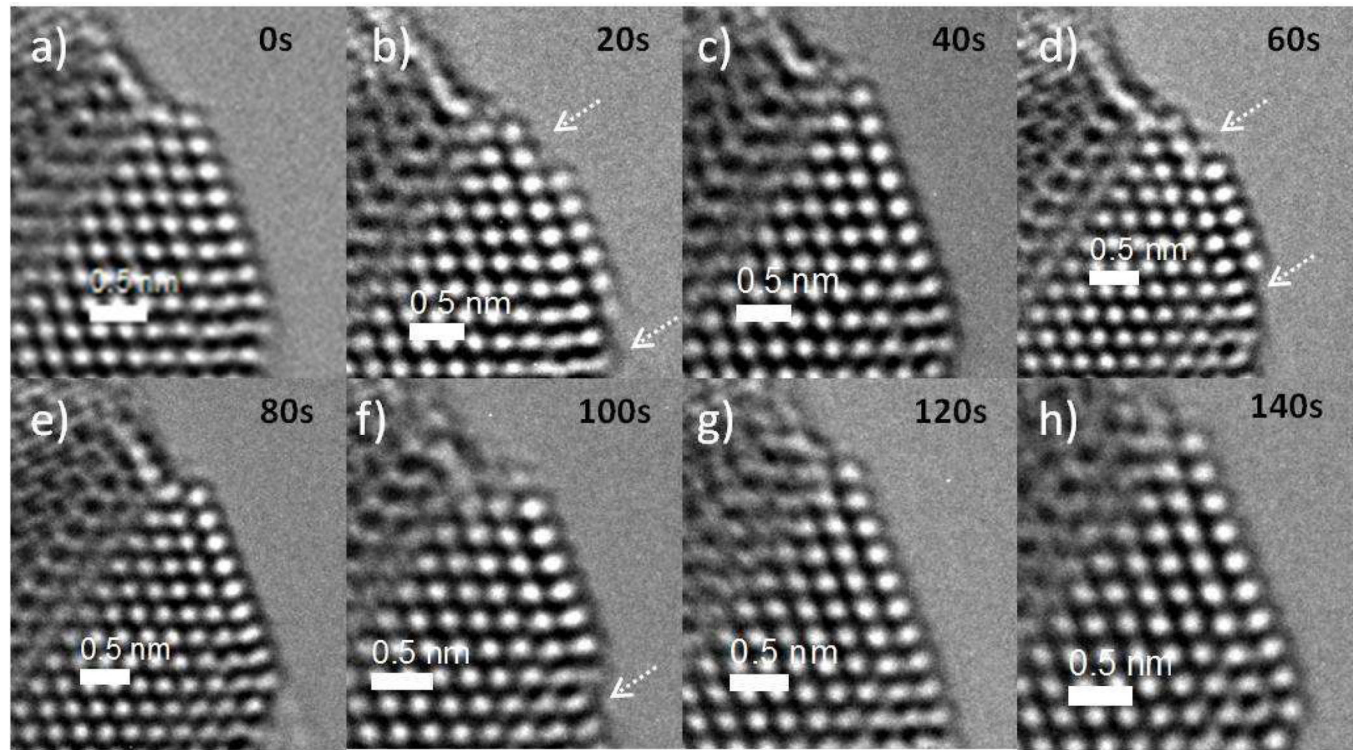


Figure 6.

Aberration corrected ultrahigh resolution images of a series of images recorded from the last layer of atoms from figure 6b, pointed by an arrow.